Numerical modeling of triaxial tests on salt rocks using a creep law with damage-induced flow

Otávio B. A. Rodrigues[1], Catarina N. A. Fernandes[1], William W. M. Lira[1]

[1]*Laboratory of Scientific Computing and Visualization, Federal University of Alagoas*
Avenida Lourival Melo Mota, S/N, Tabuleiro do Martins, 57072-970, Maceio/Alagoas, Brasil
otavio.rodrigues@lccv.ufal.br, catarina@lccv.ufal.br, william@lccv.ufal.br

Abstract. This work performs a numerical modeling of triaxial tests on salt rocks, using the Multimechanism Deformation Coupled Fracture (MDCF) creep law and the software ABAQUS. In the design of wellbores drilled on salt rocks for oil and gas exploration, computational modeling of creep is important for stability. Constitutive models describe the salt behavior and are calibrated by laboratory triaxial tests. Brazilian salt rocks are usually modelled using the double mechanism deformation, which is a good fit to several experimental tests. Yet, one of its limitations is to describe only the steady-state stage. In the literature, some more complex models represent salt creep, such as MDCF, which reproduces full creep stages and evolution of damage from the confining and deviatoric stress. The damage mechanism influences the creep strain rate, especially under low confining stresses. To achieve the proposed aim, the methodology adopted is divided into three main steps: i) numerical simulation of triaxial tests using ABAQUS; ii) customization of ABAQUS to incorporate the MDCF; iii) validation of the incorporation by comparisons with results available in the literature. The results show adequate responses for the modeled triaxial tests under several conditions. The main contribution of this work is its use as a startup step for the incorporation of the MDCF creep law in the modelling and verification of oil wellbore drilled on salt rocks stability.

Keywords: Salt rocks, Creep, Damage

1 Introduction

Salt rocks have almost zero porosity and permeability, so they are practically impermeable [1]. The existence of these rocks on topography of a region increases the probability of finding hydrocarbons reservoirs, since these structures work as traps. On the other hand, such rocks present creep, i.e., slow deformation under constant stress. When temperature is also constant, creep is divided into three phases: i) transient, represented by decrease of strain rate; ii) steady-state, where the strain stays constant; and iii) tertiary, represented by increase the strain until failure.

According to Falcão et al. [2], the creep presented by salt rocks can cause oil well closure during its drilling and, even after the well is lined, the evolution of creep deformation can continue and even cause the casing to collapse. Another problem associated to the creep of salt rocks on oil wells is their wall collapse. According to Poiate Jr. [3], this phenomenon can be caused by excess creep deformation and occurs differently in evaporites, it can cause irregularities in the caliper along the well and prison stuck pipe due to poor annular cleaning. To computationally model the creep effect, it is necessary to use constitutive laws that govern this phenomenon. Such laws can be obtained by triaxial tests on salt samples extracted from rock testimonies.

In the literature, constitutive creep laws are found for salt rocks with several purposes. Munson and Dawson [4] proposed the multimechanism deformation model, which considers steady-state creep from three mechanisms: dislocation climb, dislocation glide and undefined mechanism. Transient creep is modeled by incorporating a transient function into these mechanisms. It is a sophisticated model, whose numerical responses of triaxial tests on salt rocks were quite adequate to the experimental results. Chan et al. [5] developed the Multimechanism Deformation Coupled Fracture (MDCF), which is an extension of the multimechanism deformation [6] and it considers the creep-induced damage in the form of microcracks and voids, allowing to model the full creep curve, i.e., including the tertiary creep. Chan et al. [7] revised the MDCF and used it to obtain the creep response and

damage evolution by triaxial tests on salt rocks.

There are also constitutive laws applied to Brazilian salt rocks in the literature. Costa et al. [8] developed a creep model for salt rocks applied to drilling of oil wells in the Campos Basin. Triaxial tests were carried out on samples of salt rocks obtained from wells at Sergipe. Based on these tests, the double mechanism model was developed, which is a simplification of the Munson and Devries [9] model and considers only the steady-state creep. Firme [10] and Firme et al. [11] used two methodologies to calibrate the multimechanism deformation for Brazilian halite. They performed numerical simulations of triaxial tests, vertical wells and galleries to validate the parameters and methodologies adopted. Firme et al. [12] created the EDMT and EDMP models in order to incorporate the transient creep into the double mechanism model.

In this context, the objective of this work is perform a numerical modeling of triaxial tests on salt rocks, using the ABAQUS software and a creep law with damage-induced flow (MDCF). To achieve the proposed aim, the numerical simulation of triaxial tests and the customization of the software to incorporate the constitutive model are performed. In addition, it is presented and discussed the validation of the implementation by comparison with results available in the literature. The contributions of the work are the its use as a startup step for the incorporation of this constitutive law to the modeling and verification of oil wells stability in salt rocks, in addition to its plugging to a commercial finite element method (FEM) software.

2 Multimechanism Deformation Coupled Fracture

This section presents the MDCF equations, proposed by Chan et al. [7], using a script similar to the original work. Dislocation motions and creep-induced damage directly contribute to the inelastic strain rate. Thus, the kinetic equation of the model is given by

$$\dot{\varepsilon}_{ij} = \frac{\partial \sigma^c_{eq}}{\partial \sigma_{ij}} \dot{\varepsilon}^c_{eq} + \frac{\partial \sigma^\omega_{eq}}{\partial \sigma_{ij}} \dot{\varepsilon}^\omega_{eq}, \tag{1}$$

where $\dot{\varepsilon}_{ij}$ are the inelastic strain rate components, σ_{ij} are the stress components, σ^c_{eq}, $\dot{\varepsilon}^c_{eq}$, σ^ω_{eq} and $\dot{\varepsilon}^\omega_{eq}$ are the conjugate pairs of equivalent stress and strain rate for the dislocation and damage mechanisms, respectively. The usual convention of geomechanics is used, where compression and tension are denoted by positive and negative signs, respectively.

2.1 Equivalent stresses

The equivalent stress for the dislocation-induced flow σ^c_{eq} is the uniaxial Tresca yield stress, given by

$$\sigma^c_{eq} = |\sigma_1 - \sigma_3|\,, \tag{2}$$

where σ_1 and σ_3 are the maximum and minimum principal stresses, respectively. The equivalent stress for the damage-induced flow σ^ω_{eq} consists of three terms

$$\sigma^\omega_{eq} = |\sigma_1 - \sigma_3| - x_2 x_7 sgn(I_1 - \sigma_1) \left[\frac{I_1 - \sigma_1}{3 x_7 sgn(I_1 - \sigma_1)}\right]^{x_6} - x_1 \sigma_3 H(-\sigma_3), \tag{3}$$

where I_1 is the first invariant of the Cauchy tensor, x_i are the material constants, $sgn()$ represents the signum function and $H()$ is the Heaviside step function.

2.2 Kinetic equations for dislocation and damage-induced flows

The kinetic equation representing the strain rate due to the dislocation mechanism is based on Munson and Dawson [6] model. In this formulation, the inelastic strain rate $\dot{\varepsilon}^c_{eq}$ is given by

$$\dot{\varepsilon}^c_{eq} = F \dot{\varepsilon}_s, \tag{4}$$

where F is the transient function that describes the transient creep behavior, $\dot{\varepsilon}_s$ is the steady-state strain rate, which is the sum of three independent dislocation mechanisms $\dot{\varepsilon}_{si}$ provided by

$$\dot{\varepsilon}_{s1} = A_1 \exp\left(\frac{-Q_1}{RT}\right)\left[\frac{\sigma^c_{eq}}{G(1-\omega)}\right]^{n_1}, \tag{5}$$

$$\dot{\varepsilon}_{s2} = A_2 \exp\left(\frac{-Q_2}{RT}\right)\left[\frac{\sigma^c_{eq}}{G(1-\omega)}\right]^{n_2}, \tag{6}$$

$$\dot{\varepsilon}_{s3} = H\left[B_1 \exp\left(\frac{-Q_1}{RT}\right) + B_2 \exp\left(\frac{-Q_2}{RT}\right)\right]\sinh\left[\frac{q\left(\frac{\sigma^c_{eq}}{1-\omega} - \sigma_0\right)}{G}\right]. \tag{7}$$

Where A_i, B_i are constants, Q_i are the activation energies, T is the temperature, R is the universal gas constant, G is the transverse modulus of elasticity, n_i are the stress exponents, q is the constant stress, ω is the damage variable and σ_0 is the stress limit of the dislocation slip mechanism. The 1, 2 and 3 values assumed by the i index is the dislocation climb, undefined and glide mechanisms, respectively. The transient function F is defined as

$$F = \begin{cases} \exp\left[\Delta\left(1 - \frac{\zeta}{\varepsilon^*_t}\right)^2\right], & \zeta \leq \varepsilon^*_t \\ 1, & \zeta = \varepsilon^*_t \\ \exp\left[-\delta\left(1 - \frac{\zeta}{\varepsilon^*_t}\right)^2\right], & \zeta > \varepsilon^*_t \end{cases}, \tag{8}$$

where Δ and δ are parameters of work-hardening and recovery, respectively. ε^*_t is the transient strain limit and ζ is the hardening variable, subject to the following law of evolution:

$$\dot{\zeta} = (F-1)\dot{\varepsilon}_s. \tag{9}$$

The kinetic equation for damage-induced inelastic flow is given by

$$\dot{\varepsilon}^{\omega}_{eq} = F \exp\left[\frac{c_4(\sigma^c_{eq} - c_5)}{\sigma_0}\right]\dot{\varepsilon}^{\omega}_s, \tag{10}$$

$$\dot{\varepsilon}^{\omega}_s = c_0\left[B_1 \exp\left(\frac{-Q_1}{RT}\right) + B_2 \exp\left(\frac{-Q_2}{RT}\right)\right]\omega_0 \exp(c_3\omega)\left\{\sinh\left[\frac{c_2\sigma^{\omega}_{eq}H(\sigma^{\omega}_{eq})}{(1-\omega)G}\right]\right\}^{n_3}. \tag{11}$$

In these equations, F_ω is the transient function for the damage-induced inelastic flow, $\dot{\varepsilon}^{\omega}_s$ is the strain rate for the damage-induced flow during steady-state creep, c_0, c_2, c_3, c_4, c_5, n_3 are the material constants and ω_0 is the initial value of the damage variable. The damage evolution law is given by the following equation:

$$\dot{\omega} = \frac{x_4}{x_5}\left[\ln\left(\frac{1}{\omega}\right)\right]^{(x_4+1)/x_4}[\sigma^{\omega}_{eq}H(\sigma^{\omega}_{eq})]^{x_3} - h(T,\omega,I_1), \tag{12}$$

where x_3, x_4, x_5 are the material constants and $h(\omega, T, I_1)$ is the damage healing function , which Chan et al. [7] not determine and assumes its value as null.

2.3 Flow law

Originally the inelastic flow of the dislocation and damage mechanisms in MDCF is associative. Thus, the flow law is obtained by applying the equivalent stresses of eq. (2) and (3) in eq. (1), so that

$$\dot{\varepsilon}_{ij} = (\dot{\varepsilon}^c_{eq} + \dot{\varepsilon}^{\omega}_{eq})[b_1 s_{ij} + b_2 t_{ij}] - \dot{\varepsilon}^{\omega}_{eq}[b_4(\delta_{ij} - m_{ij}) + b_5 n_{ij}]. \tag{13}$$

In these equations, s_{ij} are the deviatoric stress components, δ_{ij} is the Kronecker delta, t_{ij} are the deviator of the square of the deviatoric stress and J_2 is the second invariant of the deviatoric tensor. The coefficients b_1, b_2, b_4 and b_5 are given by

$$b_1 = \frac{cos(2\psi)}{\sqrt{J_2}\cos(3\psi)}, \tag{14}$$

$$b_2 = \frac{\sqrt{3}}{J_2}\frac{\sin\psi}{cos(3\psi)}, \tag{15}$$

$$b_4 = \frac{x_2 x_6}{3}\left[\frac{I_1 - \sigma_1}{3sgn(I_1 - \sigma_1)}\right]^{x_6 - 1}, \tag{16}$$

$$b_5 = x_1 H(-\sigma_3), \tag{17}$$

where $m_{ij} = d\sigma_1/d\sigma_{ij}$ and n_{ij}=$d\sigma_3/d\sigma_{ij}$ are presented in Chan et al. [5] and ψ is the Lode angle.

Also, it could be admitted that the inelastic flow induced by the damage is non-associated. In these cases, it is proposed a equivalent stress $\sigma_{eq}^{\omega^*}$ is given by

$$\sigma_{eq}^{\omega^*} = |\sigma_1 - \sigma_3| - \frac{x_2 x_8}{3}[I_1 - \sigma_1] - x_1\sigma_3 H(-\sigma_3), \tag{18}$$

which is used in eq. (1). Using the new definition for equivalent damage stress in eq. (13) is also obtained b_1, b_2 and b_5, except for b_4 wich is

$$b_4 = \frac{x_2 x_8}{3}, \tag{19}$$

where x_8 is a material constant. For the associated and nonassociated formulations presented, the volumetric strain rate $\dot{\varepsilon}_{kk}$ is obtained from eq. (13) and is given by

$$\dot{\varepsilon}_{kk} = -2b_4\dot{\varepsilon}_{eq}^{\omega}, \tag{20}$$

since $s_{kk} = t_{kk} = 0$, $\delta_{kk} = 3$ and $m_{kk} = 1$. In the triaxial tests $\psi = \pm\frac{\pi}{6}$, forming indeterminacies in the coefficients b_1 and b_2. An alternative to this is to assume that

$$\frac{\partial\sigma_{eq}^{c}}{\partial\sigma_{ij}} = b_1 s_{ij} + b_2 t_{ij} = \frac{3}{2}\frac{s_{ij}}{\sigma_{eq}}. \tag{21}$$

This alternative means that the uniaxial Tresca yield stress is equal to the von Mises equivalent stress σ_{eq}. In Chan et al. [5] the components of m_{ij} are also presented for this case.

3 Numerical simulation of triaxial tests

A numerical modeling of triaxial tests using ABAQUS is defined below. So, the geometry of the specimen, the constitutive properties, the boundary conditions, the stress state, the temperature field and the finite element mesh are defined. Taking advantage of the problem's symmetry, an axisymmetric model is used whose representative section of the three-dimensional model is 1/4 of the longitudinal section of the specimen. Displacements on vertical direction are restricted at base of the model and horizontal displacements are restricted at its left side.

The model analysis is performed in three steps: geostatic, elastic and viscous. In the geostatic step, confining stresses are imposed, which simulate the original stress state of the massif. In the elastic step, the deviatoric stress is imposed on the specimen in the axial direction. In the viscous step, the creep of the salt sample is evaluated from the state of stresses induced by the confining and deviatoric stresses, as illustrated in Figure 1.

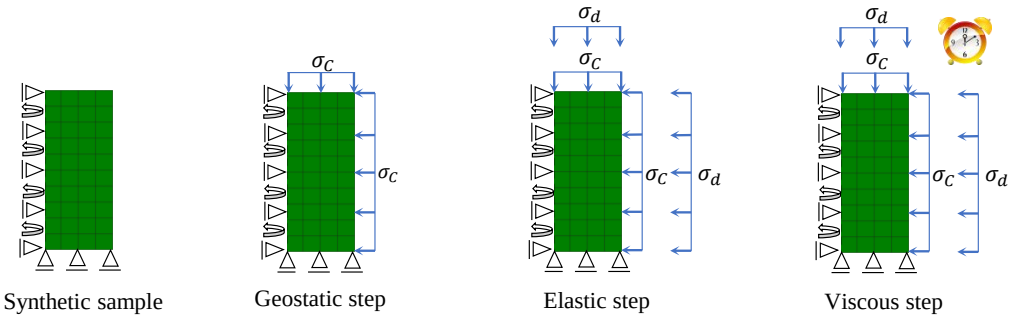

Figure 1. Numerical simulation of triaxial test. Source: adapted from [10].

4 Customizing ABAQUS to incorporate the MDCF

ABAQUS default configuration does not have MDCF. It customization is performed plugging to it a subroutine associated to this constitutive model, which is called by the software during the analysis. The subroutine is named CREEP which is implemented following the creep pattern in metals.

From the equations of the equivalent creep rate of the adopted model, which must be a function of the equivalent von Mises or Hill stress (anisotropic creep), the equivalent deviatoric $\Delta\bar{\varepsilon}^{cr}$ and volumetric strain $\Delta\bar{\varepsilon}^{sw}$ increments are incorporated to subroutine. Such increments are obtained by temporal integration methods. So, ABAQUS determines the components of creep deformation increment at each time step $\Delta\varepsilon^{cr}$ by means of

$$\Delta\varepsilon^{cr} = \frac{1}{3}\Delta\bar{\varepsilon}^{sw}\mathbf{R} + \Delta\bar{\varepsilon}^{cr}\mathbf{n}, \tag{22}$$

where $\mathbf{R}$ is a diagonal matrix with non-zero coefficients in the directions where the volumetric strains occur. When the equivalent strain rate of the creep law is a function of the von Mises equivalent stress, the components of $\mathbf{n}$ are equal to eq. (21).

The main challenge of the implementation is to adapt the directions of the MDCF strains with the subroutine, i.e., to make the relationships between the components of the tensors s_{ij}, t_{ij} in the form of $\mathbf{n}$ and $\delta_{ij}, m_{ij}, n_{ij}$ in the form of $\mathbf{R}$, see eq. (13). The first relationship is satisfied, since in triaxial tests the Tresca and von Mises stresses are equal. As for the second relation, as in these tests the stresses are of compression, the coefficient b_5 and consequently n_{ij} are null. Furthermore, the components of m_{ij} form a diagonal matrix, which agrees with the definition of $\mathbf{R}$. The deformation increments $\Delta\bar{\varepsilon}^{cr}$ and $\Delta\bar{\varepsilon}^{sw}$ are obtained based on the temporal integration of eq. (4), (10) and (20), using explicit Euler. The same method is applied to the variables ω and ζ, which are subject to laws of evolution. To obtain the principal stresses σ_1 and σ_3, necessary for the equivalent damage stress, the USDFLD subroutine is used. More details of this implementation are available in Rodrigues [13].

5 Results

Four triaxial tests (TC01, TC02, TC03 and TC04) are simulated to validate the implementation. The MDCF results for these tests are presented by Chan et al. [7]. The experiment information is provided by Fossum et al. [14]. In all tests, the samples are of WIPP (clean) salt, the specimens are cylindrical with 90 mm in diameter and 210 mm in height and the temperature is 25ºC. Table 1 shows the confining and deviatoric stresses values used by simulations.

Table 1. Numerical simulations of triaxial tests to validate implementation of the MDCF.

Simulation	Confining stress (MPa)	Deviatoric stress (MPa)
TC01	1.0	25
TC02	2.0	25
TC03	3.0	25
TC04	15.0	25

In the triaxial tests TC01 and TC02, unlike the conventional procedure in Fig. 1, the sample is confined in all directions with the magnitude of the predicted axial stress, i.e., deviatoric stress plus confining stress. The confining stress is slowly reduced until it reaches the desired value. The finite element mesh is discretized into 149 nodes and 40 elements axisymmetric elements with 8 nodes, quadratic interpolation and complete integration, as illustrated in Fig. 1. The refinement adopted for the mesh is sufficient, as in these tests the stress and strain fields are constant. The elastic properties and MDCF parameters used in the simulations are the same as Chan et al. [7].

Figures 2(a) and 2(b) present the axial and volumetric strains in TC01, TC04 and TC02, TC03, respectively, are presented. Such strains are generated considering the inelastic flow induced by damage as non-associated. In the TC01 and TC02 simulations, the usual behavior of transient, steady-state and tertiary creep is observed in the axial strains, i.e., the initial and final stretches are non-linear and intercalated by a linear behavior. In the TC03 and TC04 simulations, only the transient and steady-state creep are noticed. Volumetric strains only occur in TC01 and TC02, so that such strains are associated to tertiary creep, i.e., damage. As illustrated in Fig. 3, the damage evolution is restricted to the confining stresses, since in these tests the temperature and the deviatoric stress are equal.

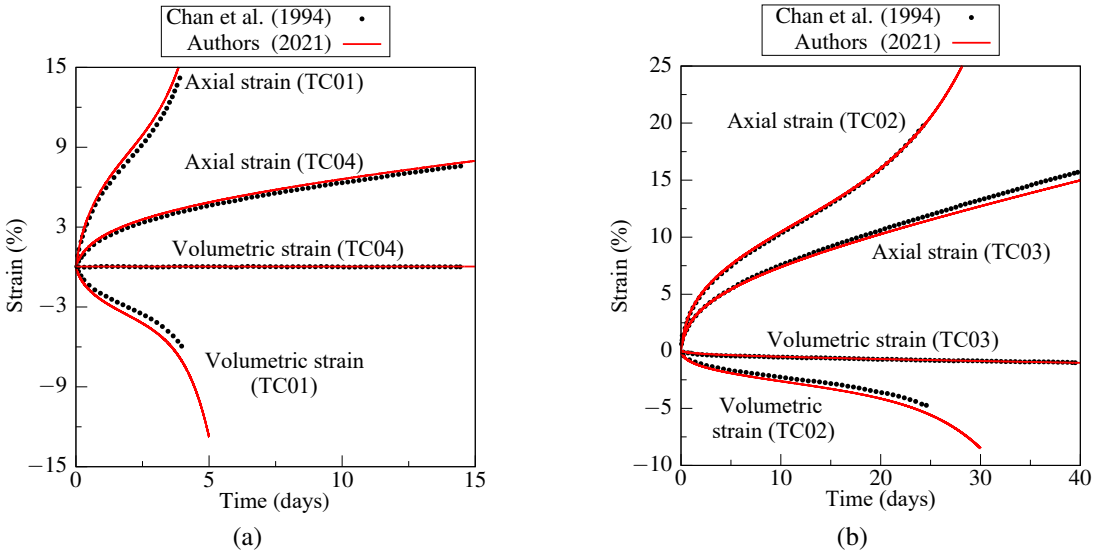

Figure 2. Axial and volumetic strains in the simulations of triaxial tests through the MDCF.

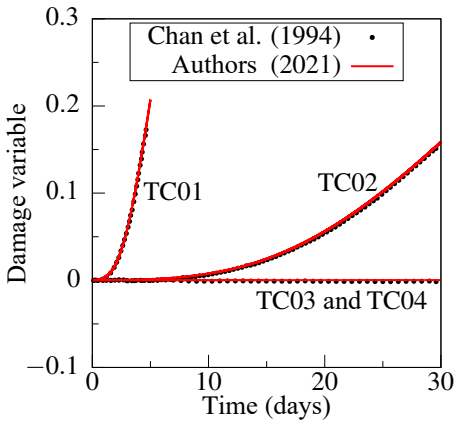

Figure 3. Damage evolution in triaxial testing simulations via MDCF.

In most simulations, the axial and volumetric strains do not agree in comparison to the reference. In the TC01 test, e.g., the axial strains obtained by the authors differ from the reference after 12 hours. On the other hand, analyzing the damage evolution, illustrated in Fig. 3, it is clear that the results are practically superimposed.

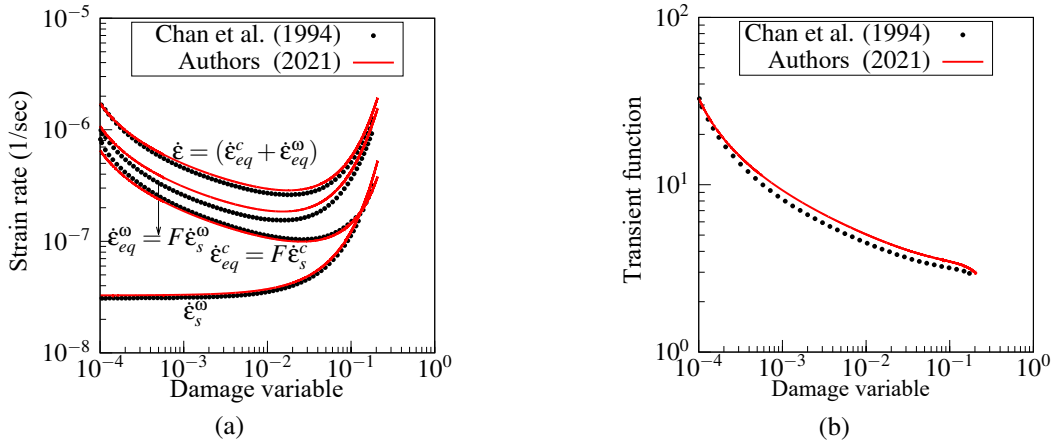

Figure 4. Strains rates and transient function in relation to damage in the TC01 simulation.

According to Fig. 4(a), the strain rates are discordant. Thus, as shown in Fig. 4(b) a possibility for errors

is associated to the transient function used. This statement is reasonable, as the axial strain curves have visually similar slopes and the transient function works as a multiplicative factor of the equivalent strain rates. In general, these disagreements can also be related to differences between ABAQUS and the reference solver. Furthermore, the temporal integration method of the variables ζ and ω adopted by Chan et al. [7] is not presented, which may be different from the one adopted in this work and may also produce differences in the results. As results have the same order of magnitude and behavior similar to the expected, the implementation is considered as validated.

6 Conclusions

This work performed a numerical modeling of triaxial tests on salt rocks using a creep law with damage-induced flow supported by the ABAQUS. Some disagreements were found in the validation of the damage model implementation, which can be ignored for the reasons mentioned. The importance of damage for the realistic modeling of creep in salt rocks is also highlighted, not only because of the aggregation of the tertiary regime, but also because of the volumetric deformations and the effect of confining stresses in the salt. So, it is possible to foresee a better safety margin for the critical problems of closure and wall collapse of oil wells in salt rocks. As a suggestion for future works, the following stand out: i) implementation of the MDCF to the ABAQUS by a UMAT subroutine, aiming at more general applications of the constitutive model such as oil wells, caverns and galleries in these rocks; ii) calibration or development of damage models for Brazilian salt rocks. A constitutive law capable of reproducing more faithfully the rocks in several stress states will make it possible to accurately predict the behavior during the construction and useful life of the oil well.

Authorship statement. The authors hereby confirm that they are the sole liable persons responsible for the authorship of this work, and that all material that has been herein included as part of the present paper is either the property (and authorship) of the authors, or has the permission of the owners to be included here.

References

[1] A. Costa and E. Poiate Jr. Rocha Salina na Indústria do Petróleo: Aspectos Relacionados à Reologia e à Perfuração de Rochas Salinas. *Sal. Geologia e Tectônica. Exemplos nas Bacias Brasileiras*, pp. 362–385, 2008.
[2] J. L. Falcão, E. P. Jr., A. M. Costa, I. A. Silva, and S. M. Eston. Perfuração em formações salinas. *Boletim técnico da Produção de Petróleo*, vol. 1, n. 2, pp. 293–307, 2007.
[3] E. Poiate Jr. *Mecânica das rochas e mecânica computacional para projeto de poços de petróleo em zonas de sal*. Tese de Doutorado, Pontifícia Universidade Católica do Rio de Janeiro, Rio de Janeiro, 2012.
[4] D. E. Munson and P. Dawson. Constitutive model for the low temperature creep of salt (with application to wipp). Technical report, Sandia Labs., 1979.
[5] K. Chan, S. Bodner, A. Fossum, and D. Munson. A constitutive model for inelastic flow and damage evolution in solids under triaxial compression. *Mechanics of Materials*, vol. 14, n. 1, pp. 1–14, 1992.
[6] D. E. Munson and P. R. Dawson. Salt-constitutive modeling using mechanism maps. vol. , 1984.
[7] K. Chan, N. Brodsky, A. Fossum, S. Bodner, and D. Munson. Damage-induced nonassociated inelastic flow in rock salt. *International journal of plasticity*, vol. 10, n. 6, pp. 623–642, 1994.
[8] A. M. Costa, E. Poiate Jr., J. L. Falcão, and L. F. M. Coelho. Triaxial creep tests in salt applied in drilling through thick salt layers in campos basin - brazil. *ISRM News Journal*, vol. 9, n. 1, pp. 14–24, 2005.
[9] D. E. Munson and K. L. Devries. Development and validation of a predictive technology for creep closure of underground rooms in salt. *7th International Congress on Rock Mechanics*, 1991.
[10] P. A. L. P. Firme. *Modelagem Constitutiva e Análise Probabilística Aplicadas a Poços em Zonas de Sal*. Dissertação de Mestrado, Pontifícia Universidade Católica do Rio de Janeiro, Rio de Janeiro, 2013.
[11] P. A. Firme, D. Roehl, and C. Romanel. An assessment of the creep behaviour of brazilian salt rocks using the multi-mechanism deformation model. *Acta Geotechnica*, vol. 11, n. 6, pp. 1445–1463, 2016.
[12] P. A. L. P. Firme, N. B. Brandao, D. Roehl, and C. Romanel. Enhanced double-mechanism creep laws for salt rocks. *Acta Geotechnica*, vol. 13, n. 6, pp. 1329–1340, 2018.
[13] O. B. A. Rodrigues. *Estudo numérico de ensaios triaxiais aplicado à perfuração de poços em rochas salinas*. Trabalho de Conclusão de Curso, Universidade Federal de Alagoas, Maceió, 2021.
[14] A. Fossum, N. Brodsky, K. Chan, and D. Munson. Experimental evaluation of a constitutive model for inelastic flow and damage evolution in solids subjected to triaxial compression. *International Journal of Rock Mechanics and Mining Sciences & Geomechanics Abstracts*, vol. 30, n. 7, pp. 1341 – 1344, 1993.